The critical end point of QCD

R. V. Gavai and Sourendu Gupta

ILGTI: TIFR

ATHIC 2008
Tsukuba, Japan
October 14, 2008

Crawling towards the continuum

- $\mu_B \neq 0$ through Taylor expansions of thermodynamic quantities.
- Before this year: state of the art lattice computations of physics for $\mu_B \neq 0$ used lattice cutoff $\Lambda = 4T \simeq 800$ MeV near T_c.
- Our earlier computation used $m_\pi \simeq 230$ MeV and spatial sizes with $LT = 2$, 3, 4 and 6. This enabled extrapolation to the thermodynamic limit, *i.e.*, $L \to \infty$.
- Now: new computations with $\Lambda = 6T \simeq 1200$ MeV near T_c (Gavai and SG, arXiv:0806.2233 [hep-lat]).
- m_π remains unchanged (230 MeV), but spatial volumes are somewhat smaller ($LT = 2$, 3 and 4). No extrapolation to $L \to \infty$ yet.
- 20000–50000 configurations (≥ 100 independent) at each coupling; stochastic determination of traces with 500 random vectors on each configuration. (Gavai and SG, Phys. Rev. D 68, 2003, 034506.)

1. Quark Number Susceptibilities
2. The Critical End Point
3. Series sums and Padé resummations
4. Experiment

Outline

1. Quark Number Susceptibilities
2. The Critical End Point
3. Series sums and Padé resummations
4. Experiment

What is a QNS?

Taylor coefficient of the pressure in $N_f = 2$ QCD is

$$P(T, \mu_u, \mu_d) = \sum_{n_u, n_d} \frac{1}{n_u! n_d!} \chi_{n_u, n_d}(T) \mu_u^{n_u} \mu_d^{n_d},$$

and, since the two quark flavours are degenerate, $\chi_{n_u,n_d} = \chi_{n_d,n_u}$. Trade $\mu_{u,d}$ for $\mu_{B,Q}$. Then

$$\chi_B = \frac{2}{9}(\chi_{20} + \chi_{11}) = 2\chi_{BQ} \qquad \chi_Q = \frac{1}{9}(5\chi_{20} - 4\chi_{11}).$$

Transforming to μ_{B,I_3}, one has

$$\chi_{BI_3} = 0, \qquad \chi_{I_3} = \frac{1}{2}(\chi_{20} - \chi_{11}).$$

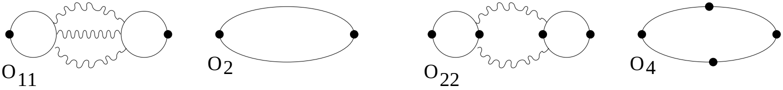

Off-diagonal QNS

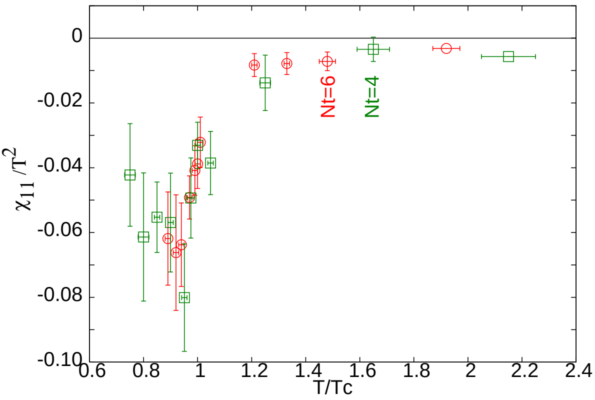

Sees only $\langle O_{11} \rangle$. No evidence for lattice spacing effects.

Diagonal QNS

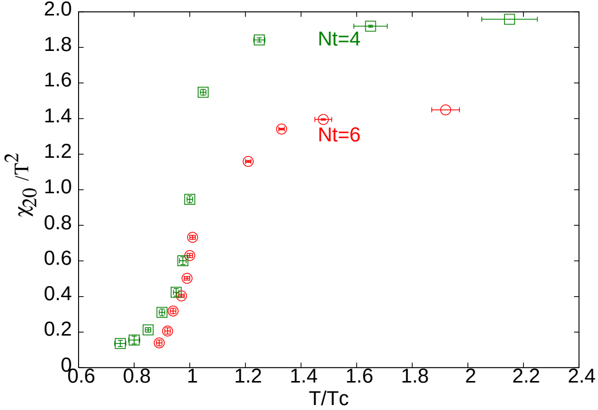

Sees $\langle O_{11} \rangle$ and $\langle O_2 \rangle$. Second expectation value is cutoff dependent. Also, has a cross over. We look at its susceptibility $\langle O_{22} \rangle_c$ to identify T_c.

"Susceptibility" of QNS: $\langle O_{22} \rangle_c$— 4th order QNS

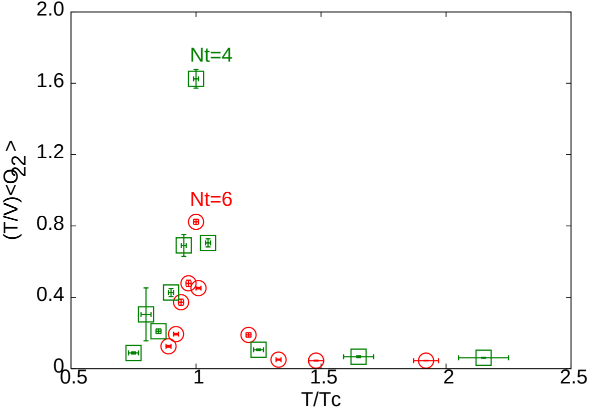

Peak at the same coupling as peak of χ_L. Within the 1% precision of T/T_c, the two quantities peak at the same coupling. See Gavai and Gupta, PR D72 (2005) 054006.

Diagonal fourth-order QNS

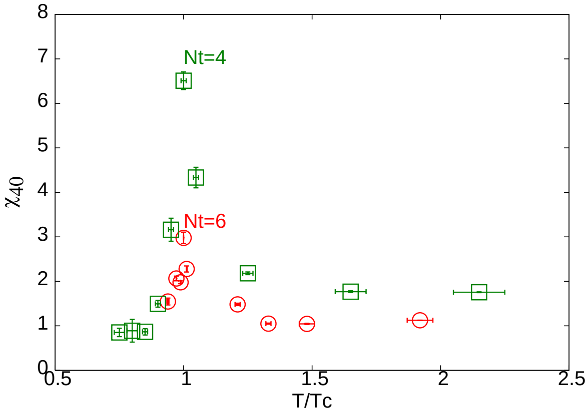

Non-zero for $T > T_c$. Has contribution from $\langle O_4 \rangle$, which has non-vanishing value for the ideal gas.

The operator O_4

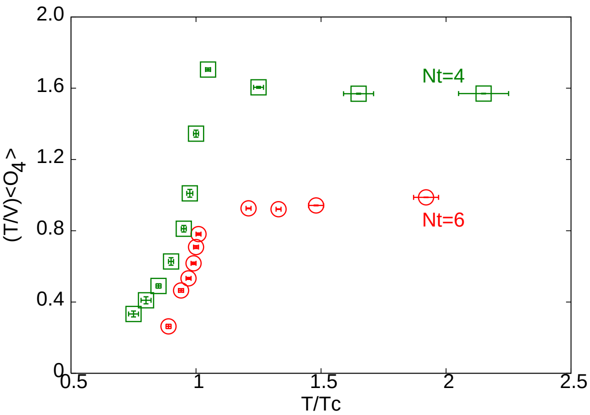

Rapid cross over from a small value in the hadronic phase to a non-vanishing value for the ideal gas.

"Susceptibility" of O_4: $\langle O_{44} \rangle_c$— 8th order QNS

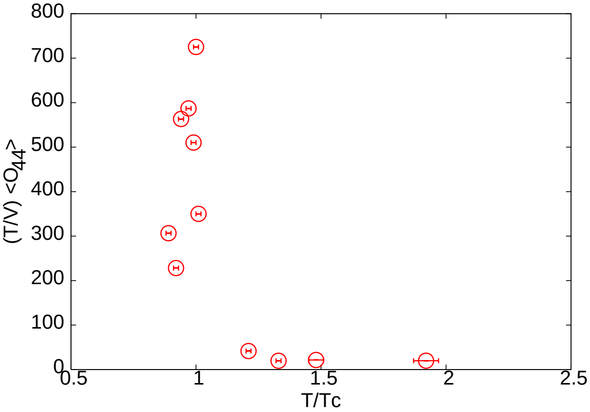

This quantity peaks at the same coupling as χ_L and $\langle O_{22} \rangle_c$. Within the precision of our measurement there is no dependence of the cross over coupling on these observables.

The operator O_6— 6th order QNS

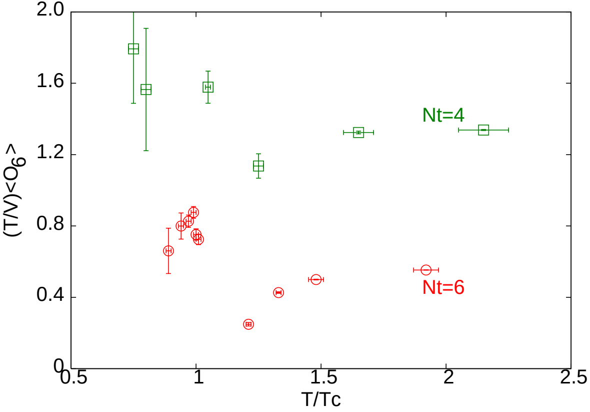

The operator expectation value $\langle O_6 \rangle$ has structure below T_c and hence its "susceptibility" cannot be used to probe the cross over coupling. Similar observation for $\langle O_8 \rangle$.

Outline

1 Quark Number Susceptibilities

2 The Critical End Point

3 Series sums and Padé resummations

4 Experiment

Finite size effects

- At critical point correlation length becomes infinite, appropriate susceptibilities diverge and free energy becomes singular ... in the infinite volume limit (van Hove's theorem).
- No numerical computation ever performed on infinite volumes.
- Deduce the existence of a critical point through extrapolations: finite size scaling (FSS) well developed for direct simulations.
- Example: peak of susceptibility scales as power of volume. Smaller effect: position of peak shifts from its infinite volume position by a different power of volume—

$$\chi_{max}(L) \propto L^p, \qquad T_c(L) = T_c - a/L^q, \qquad (p, q > 0).$$

- FSS not well developed for series expansions; some aspects are known.

Series expansions

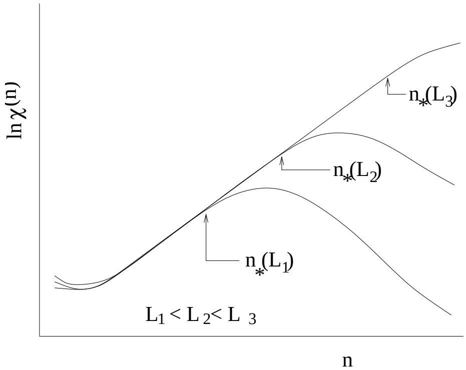

For the divergent quantity: $\chi_B(T, \mu_B) = \sum_n \chi^{(n)}(T)\mu_B^n$, the leading finite volume effects in the series coefficients.

$N_t = 4$

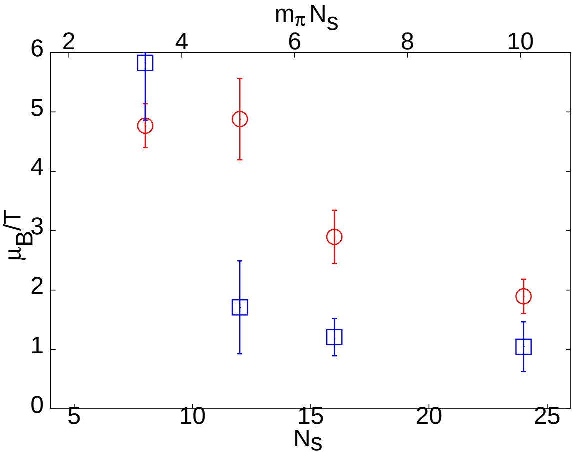

At fixed $T/T_c \simeq 0.95$. Circles: ratio of order 0 and 2; boxes: ratio of order 2 and 4. Gavai and SG, Phys. Rev. D 71, 2005, 114014.

$N_t = 6$: Radius of convergence

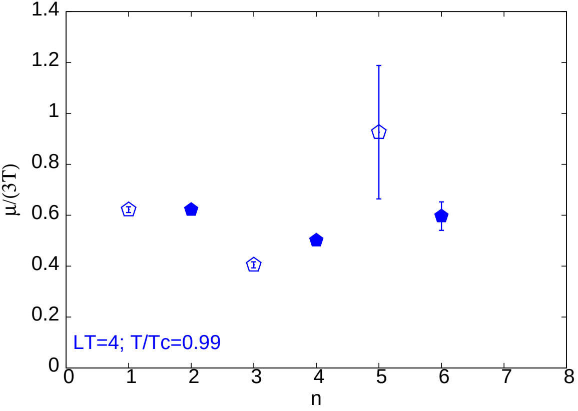

Filled symbols: $(\chi^{(0)}/\chi^{(n)})^{1/n}$. Open symbols: $\sqrt{\chi^{(n-1)}/\chi^{(n+1)}}$.

$N_t = 6$: Radius of convergence

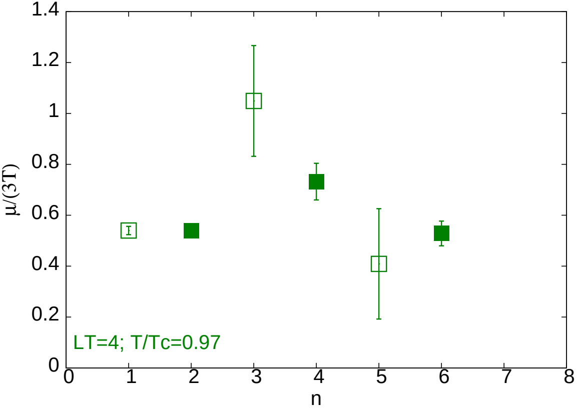

Filled symbols: $(\chi^{(0)}/\chi^{(n)})^{1/n}$. Open symbols: $\sqrt{\chi^{(n-1)}/\chi^{(n+1)}}$.

$N_t = 6$: Radius of convergence

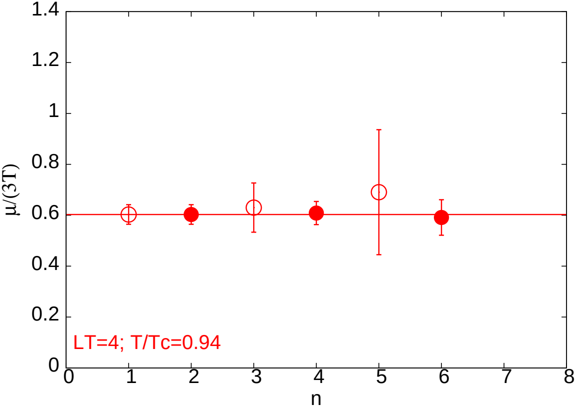

Filled symbols: $(\chi^{(0)}/\chi^{(n)})^{1/n}$. Open symbols: $\sqrt{\chi^{(n-1)}/\chi^{(n+1)}}$.

$N_t = 6$: Finite size scaling

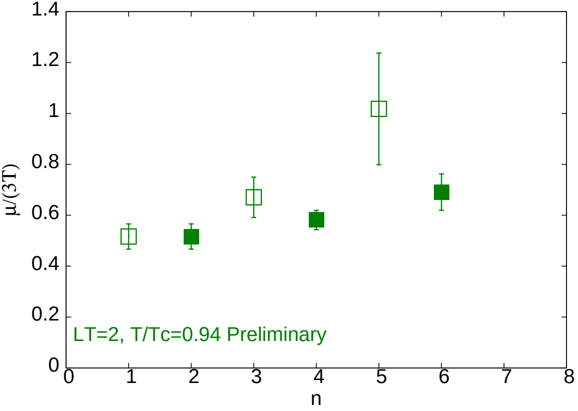

Filled symbols: $(\chi^{(0)}/\chi^{(n)})^{1/n}$. Open symbols: $\sqrt{\chi^{(n-1)}/\chi^{(n+1)}}$.

$N_t = 6$: Finite size scaling

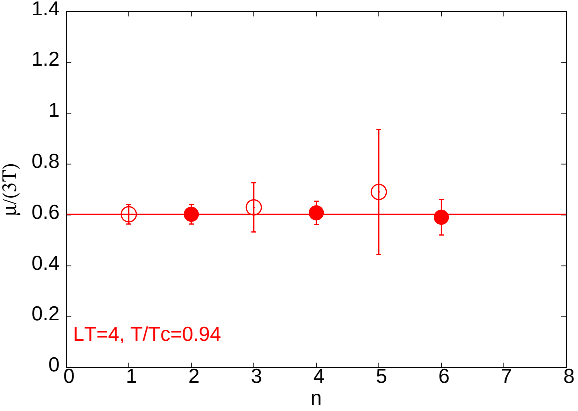

Filled symbols: $(\chi^{(0)}/\chi^{(n)})^{1/n}$. Open symbols: $\sqrt{\chi^{(n-1)}/\chi^{(n+1)}}$.

“Kurtosis” and radius of convergence

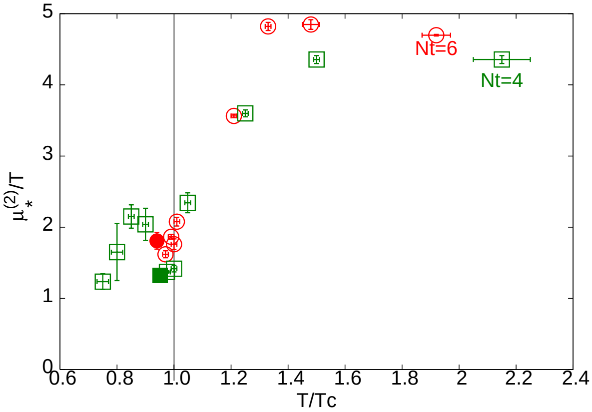

Plot of $\sqrt{12\chi^{(2)}/\chi^{(4)}}$. Lattice spacing dependence quantifies possible systematic errors. Related to Kurtosis: experimental measurement possible.

Critical end point

- Multiple criteria agree:
  - Small window in T where all the coefficients are positive.
  - Stability of radius of convergence with order and estimator
  - Finite size effects follow correct trend; more planned for the future.
  - Pinching of the radius of convergence with T: (experimental measurement of Kurtosis?)
- This gives

$$\mathbf{\frac{T^E}{T_c} = 0.94 \pm 0.01} \qquad \text{and} \qquad \mathbf{\frac{\mu_B^E}{T^E} = 1.8 \pm 0.1}$$

with $Nf = 2$ when $m_\pi/m_\rho \simeq 0.3$ at a finite volume with $LT = 4$ and lattice cutoff of $a = 1/6T^E$.

- For a lattice cutoff of $a = 1/4T^E$ at the same renormalized quark mass and on the same volume we had found a similar value for T^E/T_c and $\mu_B^E/T^E = 1.3 \pm 0.3$. Extrapolation to $L \to \infty$ reduced this to 1.1 ± 0.1.

Outline

1. Quark Number Susceptibilities
2. The Critical End Point
3. Series sums and Padé resummations
4. Experiment

Fluctuations of Baryon number

Suggestion by Stephanov, Rajagopal, Shuryak; Asakawa, Heinz, Muller; Jeon, Koch

$$P(\Delta B) = \exp\left(-\frac{(\Delta B)^2}{2VT\chi_B}\right).$$

Extrapolate χ_B to finite chemical potential: peak at T_c?

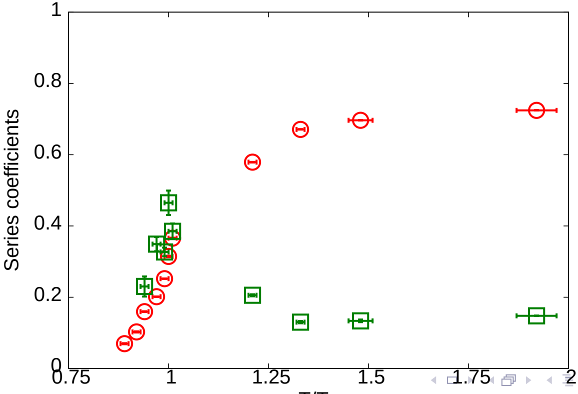

Sum the series

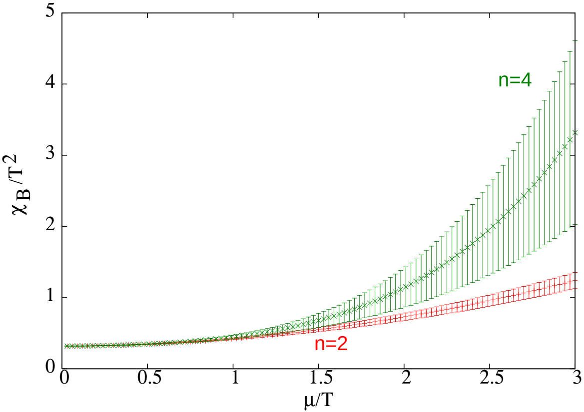

Summing the series never shows critical behaviour: sum is a polynomial and smoothly behaved. The sum peaks at T_c: incorrect (see SG, SEWM 2006).

Critical fluctuations

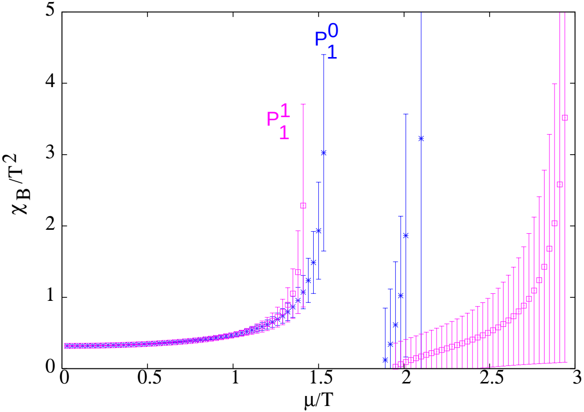

Use Padé approximants for the extrapolations: divergence only at the critical end point. Error propagation requires care: see arXiv:0806.2233 [hep-lat].

Outline

1. Quark Number Susceptibilities
2. The Critical End Point
3. Series sums and Padé resummations
4. Experiment

Experimental measurement of critical index

Near the critical point

$$\chi^{(2)} \propto |\mu - \mu_B^E|^{-\gamma}, \quad \chi^{(4)} \propto |\mu - \mu_B^E|^{-\gamma-2} \qquad (\gamma > 0).$$

The Kurtosis diverges:

$$K = -1 + \frac{\chi^{(4)}}{3[\chi^{(2)}]^2} \propto |\mu - \mu_c|^{\gamma-2};$$

(recall that $P = P_0 + p|\mu - \mu_c|^{-\gamma+2}$ is non-analytic but non-divergent). Along freezeout trajectory in an energy scan, the Kurtosis is non-monotonic. Should be visible in experiment. Look for non-Gaussian (E-to-E) fluctuations. Big question: what can hide non-Gaussian fluctuations?
Exciting possibility: **can one measure a critical index in experiments**?